Available on line www.jocpr.com

Journal of Chemical and Pharmaceutical Research

J. Chem. Pharm. Res., 2011, 3(3):25-37

ISSN No: 0975-7384
CODEN(USA): JCPRC5

Comparative structural and vibrational studies of 6-amino purine (Guanine) and its radical species using density functional theory

Rashmi Singh*, M. Kumar, P. Singh and R A Yadav

Lasers and Spectroscopy Laboratory, Department of Physics, Banaras Hindu University, Varanasi, India

ABSTRACT

Guanine (G) is one of the most important nucleic acid bases (NAB) occurring in both DNA and RNA. In addition to being the largest NAB, it has also the most complex tautomeric equilibria. It is very important to understand the properties of the guanine base of DNA as thoroughly as possible since it is the most frequently involved site in the processes of mutation and cancer. The equilibrium geometries, APT charges, fundamental vibrational frequencies along with their corresponding intensities in IR spectrum, Raman activities and depolarization ratios of the Raman bands for the neutral and its radical species (G, G^{+}, G^{-}) of the guanine molecule were computed by density functional B3LYP method with 6-311++G (d, p) basis sets using Gaussian-03 software. The thermodynamic functions of the title compounds were also performed at the same basis sets. The calculations predicted the G molecule as well as the radical anionic species of G to possess planar structures with C_1 point group symmetry whereas the radical cationic species of G possesses C_s point group symmetry. The properties of the radical cations that are generated from the neutral neleobase molecules during the certain processes helps in understanding the nuclei acids in different environments and conditions. The radical anions are intermediates in a numbers of chemical reactions. Therefore data of their structures are useful for studying the mechanism and kinetics.

Keywords: DFT Calculations; APT Charges; guanine and its radical species; applications.

INTRODUCTION

IR spectroscopy analysis of guanine the Ar-matrix has suggested the presence of both keto and enol tautomers in the equal proportion [1]. The stability of keto-N_7H tautomers is most stable in gas phase but in the environment (water solution) stability is shifted towards the keto-N_9H tautomers [2]. The location of the initial charges in DNA and RNA largely affect and govern the creation of the neutral nucleotide radicals, which are formed by protonation of the radical anions and deprotonation of the radical cations [3-5]. Exposure of DNA and RNA to high-energy radiation is expected to lead formation of anions and cations at various sites within the strand. The relative stability of guanine tautomers is found to be significantly influenced by the molecular environment [6]. The properties of the radical cations that are generated from the neutral neleobase molecules during the certain processes helps in understanding the nucleic acids in different environments and conditions. The radical anions are intermediates in a numbers of chemical reactions. Therefore data of their structures are useful for studying the mechanism and kinetics.

The crystal structure of the neutral N_9H guanine has been taken by experimental data of Bugg and Thewalt [7]. The studies of the radical ions of keto-N_9H guanine in gas phase have been made by Zhang et al. [8]. Several studies of IR and Raman spectra of the N_9H guanine derivatives have been published [9-14]. Florian has been calculated the scaled quantum mechanical force fields and vibrational spectra of solid-state nucleic acid constituents [15]. The theoretical wave numbers of guanine predicted good agreements with earlier observed wave numbers by Nishimura et al. [16].

The frequency calculations indicated that they are now at energy minima. In this way, the stationary points of all the structures were obtained at the same theoretical level of B3LYP/6-311++G** which is a prerequisite for the geometric and energetic comparisons. G^+ favors the planar geometrical structure while the neutral G and G^- is non-planar symmetric structure.

Computational detail

The DFT calculations were carried out to compute the optimized molecular geometries, APT charges and fundamental vibrational frequencies along with their corresponding intensities in IR spectrum, Raman activities and depolarization ratios of the Raman bands for the neutral G as well as their radical species (G, G^+, G^-) using Gaussian-03 [17]. For the radical cations of the both molecules, the input structures are taken from the geometries of their corresponding neutral molecules optimized at the B3LYP/6-311++G** level and the DFT calculations were performed using the B3LYP/6-311++G** level by taking the charge as +1 and multiplicity as 2. For the computations of different parameters of our interest for the anions of G molecules computations were performed at the B3LYP/6-311++G** level by taking the input structures from the geometries of its corresponding neutral molecules, as for the anion, and the charge as -1 and multiplicity as 2. The frequency calculations indicated that they are now at energy minima. In this way, the stationary points of all the structures were obtained at the same theoretical level of B3LYP/6-311++G** which is a prerequisite for the geometric and energetic comparisons. The geometries were optimized by minimizing the energies with respect to all the geometrical parameters without imposing any molecular symmetry constraints. The assignments of the normal modes of vibration for all the three molecules have been made by visual inspection of the individual mode using the GaussView software [18].

Table-1 Optimized geometrical parameters[a] of G, G$^+$ and G$^-$ molecules

Definitions	G		G$^+$	G$^-$
	Cal	Exp[b]		
r (N_1-C_2)	1.370	1.371	1.358	1.376
r (C_2-N_3)	1.308	1.315	1.358	1.317
r (N_3-C_4)	1.356	1.364	1.309	1.350
r (C_4-C_5)	1.393	1.382	1.439	1.396
r (C_5-C_6)	1.439	1.405	1.461	1.438
r (C_6-O_{12})	1.213		1.198	1.221
r (C_6-N_1)	1.440	1.398	1.441	1.428
r (N_7-C_5)	1.380	1.405	1.333	1.384
r (C_8-N_7)	1.304	1.314	1.337	1.306
r (N_9-C_8)	1.385	1.369	1.366	1.382
r (N_9-C_4)	1.369	1.364	1.374	1.371
r (C_2-N_{10})	1.375		1.328	1.362
r (N_9-H_{14})	1.009		1.013	1.013
r (C_8-H_{13})	1.080		1.081	1.080
r (N_1-H_{11})	1.012		1.016	1.017
r (N_{10}-H_{16})	1.009		1.010	1.020
r (N_{10}-H_{15})	1.009		1.012	1.014
α(C_8-N_9-C_4)	106.7		106.7	106.8
α(C_8-N_9-H_{14})	127.7		127.1	127.2
α(C_4-N_9-H_{14})	125.6		126.2	125.9
α(N_9-C_8-H_{13})	121.7		122.4	121.2
α(N_9-C_8-N_7)	112.6		113.2	112.8
α(H_{13}-C_8-N_7)	125.7		124.4	125.9
α(C_8-N_7-C_5)	104.8		104.8	104.7
α(N_7-C_5-C_6)	130.4		130.5	130.8
α(N_7-C_5-C_4)	110.8		111.4	110.8
α(C_6-C_5-C_4)	118.7		118.2	118.4
α(C_5-C_6-O_{12})	131.3		129.3	130.4
α(C_5-C_6-N_1)	109.5		110.2	109.9
α(O_{12}-C_6-N_1)	119.2		120.6	119.7
α(C_6-N_1-H_{11})	113.5		113.6	114.7
α(C_6-N_1-C_2)	126.5		126.1	126.6
α(H_{11}-N_1-C_2)	120.0		120.4	118.7
α(N_1-C_2-N_{10})	117.0		120.3	117.1
α(N_1-C_2-N_3)	123.4		123.2	122.8
α(N_{10}-C_2-N_3)	119.6		116.5	120.1
α(C_2-N_{10}-H_{16})	118.2		123.4	119.3
α(C_2-N_{10}-H_{15})	113.8		118.1	115.2
α (H_{16}-N_{10}-H_{15})	114.7		118.5	114.6
α (C_2-N_3-C_4)	112.9		114.2	113.0
α(N_9-C_4-C_5)	105.0		103.9	104.9
α (N_9-C_4-N_3)	125.9		127.9	125.9
α(C_5-C_4-N_3)	129.1		128.2	129.2

[a] *Bond lengths (r) in Å and Angles (°) in degrees*

[b] *Ref. [7]*

Fig. 1

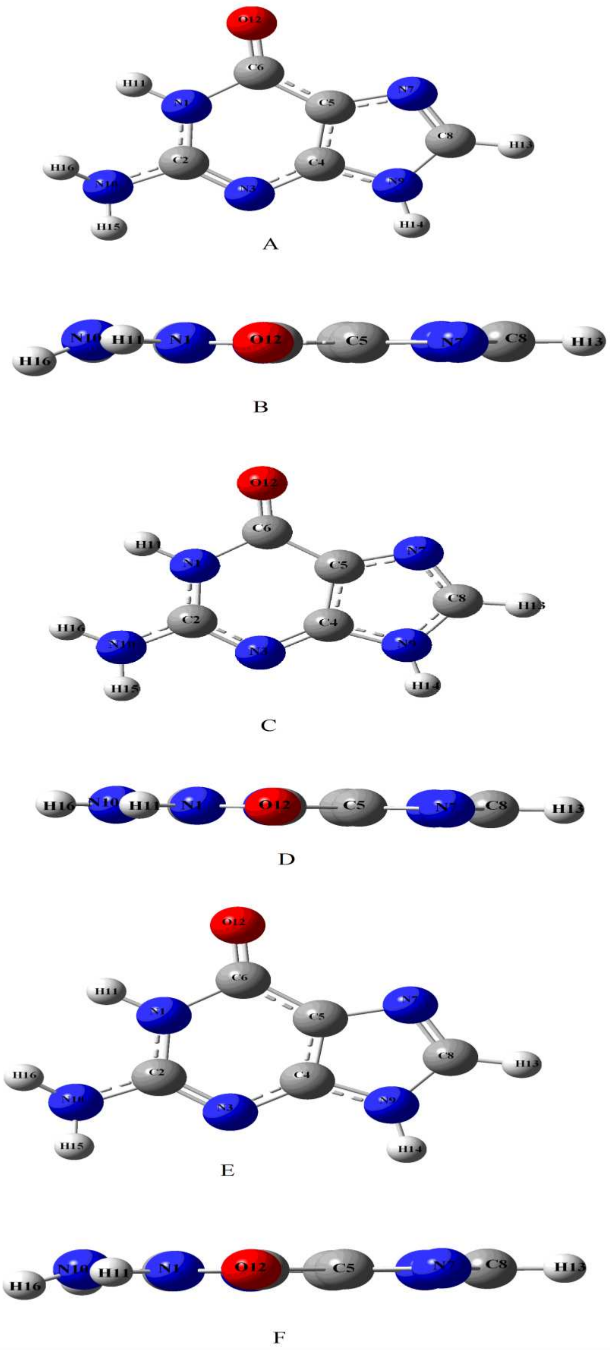

A- Front View, numbering scheme and the optimized structures of the G molecule.
B- Lateral View, numbering scheme and the optimized structures of the G molecule.
C- Front View, numbering scheme and the optimized structures of the G^+ molecule.
D- Lateral View, numbering scheme and the optimized structures of the G^+ molecule.
E- Front View, numbering scheme and the optimized structures of the G^- molecule
F- Lateral View, numbering scheme and the optimized structures of the G^- molecule.

RESULTS AND DISCUSSION

3.1 Molecular structure

The optimized geometrical parameters for the G molecule and its corresponding radicals calculated at the B3LYP/6-311++G** level along with the experimental parameters for the G molecule are collected in Table-1. The numbering schemes for these molecules are shown in Figs.1. The ab initio calculations predicted the neutral G species and its radical anion possess planar structures with C_1 point group symmetry while the radical cations of G possess C_s point group symmetry. We can be seen from the Table-1 and Fig-2A, small differences in geometries of the anionic and cationic species from the neutral species. APT charges at atomic sites of the G and its radical species are collected in Table-2 and also a graph of APT charges of studies species in Fig-2B.

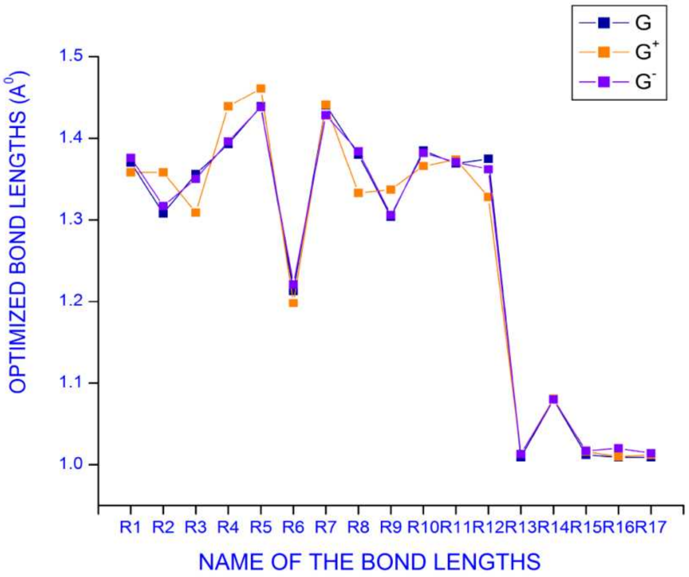

Fig. 2 A: Variations of Optimized Bond length of the G and its ionic radicals

Table-2 APT atomic charges of G, G^+ and G^- at the B3LYP/6-311++G level.**

Atom	G	G^+	G^-
N_1	-0.6518	-0.6836	0.7221
C_2	1.1402	1.2689	-2.0295
N_3	-0.8282	-0.6332	1.5690
C_4	0.6533	0.4648	-1.1863
C_5	-0.2586	0.2111	0.3736
C_6	1.2309	0.9241	-0.2532
N_7	-0.3645	-0.5540	0.2039
C_8	0.1833	0.4907	0.3321
N_9	-0.3946	-0.4592	0.6199
N_{10}	-0.8054	-0.7978	1.9519
H_{11}	0.2059	0.2476	-0.4646
O_{12}	-0.8875	-0.5660	-0.1875
H_{13}	0.0736	0.1511	-0.0806
H_{14}	0.2519	0.3103	-0.8957
H_{15}	0.2278	0.3174	-0.4846
H_{16}	0.2236	0.3078	-1.1906

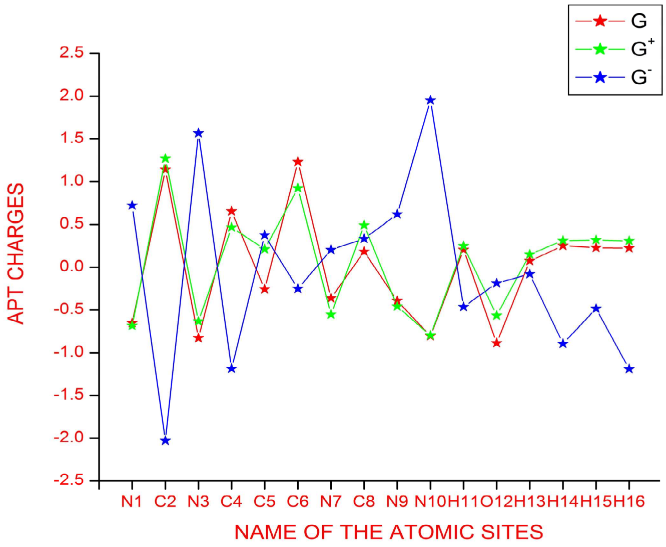

Fig. 2 B: APT Charges on the atomic sites of the G and its ionic radicals.

From the calculations it is found to the bond lengths of the N_1-C_2, N_3-C_4, N_7-C_5, N_9-C_8 and C_2-N_{10} bonds are lower in magnitudes for the cationic species of guanine and other bond lengths of the N-C bond of purine ring have found to be lengthened. In case of the guanine anionic species G^- length of the N_1-C_2 and N_3-C_2 bonds are lengthened by lower magnitude and one bonds N_1-C_6 is shortened by 0.012 as compared to the neutral G molecule. The bond lengths are shortened by 0.006 and 0.013 of the N_3-C_4 and C_2-N_{10} bonds due to the radicalization process. Redistribution of the electrons on the G^+ species the atomic charges of each atom are slightly increases (Table-2 and Fig-2B). Due to the increase of atomic charges of all H atoms, the lengths of all N-H and C-H bonds slightly increases in the G^+ species as compared to its neutral molecule (Fig-2A and 2B). In case of the G^- radical all H atoms get negative charges, due to this the lengths of the N-H bonds increases except the C-H bond length as compared to the G species. The C-C bond length of the ring for the G^+ radical increases than that of the G molecule due to the radicalization process C_5 sites get positive charges which repeals the C_6 atom. The C=O bond length shorter for the G^+ radical due to the positive charge on the C_5 and C_6 atoms both repeals to each other and the O atom pulls very easily C_6 towards itself. For the G^- radical its value longer as compared to its neutral G molecules due to the attaching of one electron the C_6 site gets negative charge and this causes the increases of the bond length of the C=O bond in the G^- radical.

3.2 Vibrational Analysis

Here, I have described only those frequencies which show major differences after calculations. The magnitude of the calculated frequency of non-planer ring deformation mode 5, 12 and 14 have to found increase for the G^+ radical than those of the G molecule with the depolarized Raman bands. However, nearly equal magnitudes with the G for the G^- ions with increased IR intensity and Raman activity. It is notice for the magnitudes of the frequencies 28 and 31 increase in the G^+ radical but for mode 30 and 34 decrease as compared to the G molecule. The magnitude of planer ring deformation mode 35 decreases by 30 cm^{-1} and depolarization ration increases for the G^+ radical than those in the G molecule. For the anionic species the G^- radical the value of calculated frequency is nearly same but the IR intensity and Raman activity increases by a large factor.

Table-3 Calculated fundamental frequencies[a] of Guanine and its radicals

S. No.	G	G^+	G^-	Assignments
1	136 (3.20, 0.15) 0.74	119 (3.21, 0.02) 0.75	137 (9.76,1723.58) 0.75	ϕ(ring) a″ Butter fly mode
2	156 (1.38, 0.09) 0.56	148 (0.01,0.22) 0.75	163 (17.83,1839.79) 0.66	ϕ(ring) a″
3	196 (11.25, 0.12) 0.62	201 (12.58, 0.416) 0.75	198 (2.62,6542.13) 0.62	ϕ(ring) a″
4	318 (15.51, 1.28) 0.62	320 (2.102, 1.85) 0.55	319 (14.31, 240.31) 0.29	α (ring) a′
5	328 (58.45, 0.32) 0.17	458 (77.32, 0.18) 0.75	372 (761.02,57113.69) 0.72	τ (NH_2) a″
6	335 (11.75, 2.96) 0.69	345 (5.84, 3.09) 0.73	338 (1.68, 1045.55) 0.73	β(C-NH_2) a′
7	356 (1.66, 0.62) 0.68	309 (8.45, 0.16) 0.75	350 (21.15, 38064.01) 0.74	ϕ(ring) a″
8	488 (7.48, 4.90) 0.45	477 (4.05, 7.95) 0.32	490 (11.97,5713.73) 0.48	α (ring) a′
9	526 (19.43, 3.86) 0.71	515 (0.22, 5.11) 0.63	529 (33.18, 2901.89) 0.71	α (ring) a′
10	534 (81.12, 0.55) 0.75	635 (74.66, 0.08) 0.75	523 (27.21, 125202.34) 0.75	γ (N_1H) a″
11	544 (260.17, 1.38) 0.74	540 (45.37, 0.25) 0.75	452 (130.59,57853.06) 0.66	ω (NH_2) a″
12	6 594 (79.28, 0.96) 0.74	682 (84.24,0.60) 0.75	602 (153.42, 55924.31) 0.54	γ (N_1H) a″
13	624 (8.03, 28.10)	616 (3.13, 28.75) 0.12	625 (17.89,6775.08) 0.54	α (ring) a′
14	660 (3.08, 0.36)	557 (162.35, 1.18) 0.75	660 (46.00,14383.56) 0.62	ϕ(ring) a″
15	668 (21.53, 0.42)	668 (12.67, 2.60) 0.75	665 (160.96, 23339.44) 0.44	β(C=O) a′
16	696 (38.99, 0.13)	628 (2.27, 0.66)	688 (24.97, 3792.69)	ϕ(ring) a″

	0.71	0.75	0.50	
17	734 (5.47, 0.13) 0.51	726 (0.45, 0.19) 0.75	723 (123.22, 22505.83) 0.39	γ (C-NH$_2$) a″
18	777 (21.54, 1.46) 0.72	769 (15.17, 0.31) 0.75	778 (5.37, 2866.90) 0.75	γ (C=O) a″
19	819 (11.79,0.79) 0.73	887 (4.2882, 0.2287) 0.7498	818 (2.74, 115060.74) 0.75	γ (CH) a′
20	835 (8.66,1.76) 0.67	833 (8.21, 1.34) 0.54	831 (42.21, 3395.46) 0.44	ν (ring) a′
21	948 (7.64,6.32) 0.29	918 (3.19, 6.22) 0.69	944 (289.17, 2316.09) 0.64	α (ring) a′
22	1044 (9.44, 3.73) 0.26	1039 (1.22, 2.92) 0.28	1039 (30.70, 2637.94) 0.31	ν (ring) a′
23	1064 (37.84, 3.46) 0.21	1053 (36.98 , 5.23) 0.1024	1081 (20.71, 12501.18) 0.43	ν (ring) a′ + ρ (NH$_2$)
24	1069 (18.83, 4.09) 0.11	1086 (5.48, 20.83) 0.2181	1062 (1913.54, 33025.19) 0.70	ν (ring) a′ + ρ (NH$_2$) + β(N$_1$H) a′
25	1136 (33.97,3.44) 0.34	1099 (65.51,20.72) 0.28	1131 (81.04, 17898.37) 0.65	ρ (NH$_2$) a′
26	1169 (25.71,1.99) 0.73	1165 (24.93,1.82) 0.61	1167 (77.36, 1852.35) 0.68	ν (ring) a′ + β(CH)
27	1304 (1.61,20.92) 0.22	1230 (40.24,42.28) 0.34	1301 (555.46, 23140.99) 0.36	β(CH) a′
28	1332 (71.32, 7.50) 0.69	1380 (179.13, 48.08) 0.58	1332 (210.18, 30830.15) 0.38	β(N$_1$H) a′
29	1355 (15.62, 7.76) 0.74	1410 (169.76, 20.27) 0.69	1349 (47.70,1247.06) 0.51	ν (ring) a′ + β(CH) a′
30	1382 (13.99, 90.09) 0.33	1422 (7.23, 16.73) 0.19	1379 (175.53,17352.34) 0.63	β(N$_9$H) a′ + ν (ring) a′
31	1434 (23.76,15.60) 0.70	1353 (25.05 , 57.61) 0.60	1420 (251.42, 22135.93) 0.18	ν (ring) a′
32	1508 (2.67,133.47) 0.18	1481 (14.01, 16.76) 0.60	1507 (42.48, 7006.27) 0.6645	ν (ring) a′
33	1554 (80.71,29.59) 0.45	1527 (105.39,16.70) 0.11	1547 (365.94,19564.37) 0.61	ν(C-NH$_2$) a′ + ν (ring) a′
34	1603 (184.33, 83.52) 0.36	1645 (240.95,294.51) 0.33	1618 (837.21, 54603.71) 0.16	ν (ring) a′

35	1614 (237.77, 41.42) 0.19	1592 (48.35, 41.96) 0.26	1564 (6875.45, 694028.91) 0.38	ν (ring) a′ + σ (NH$_2$) a′
36	1661 (421.66, 38.45) 0.21	1683 (458.66,34.18) 0.24	1581 (1571.25, 47413.15) 0.20	σ (NH$_2$) a′
37	1792 (758.29, 52.69) 0.40	1788 (238.55, 215) 0.37	1757 (404.52, 13170.31) 0.34	ν (C=O) a′
38	3242 (0.27 , 126.85) 0.28	3250 (19.00, 123.36) 0.27	3226 (105.02, 34799.84) 0.45	ν (CH) a′
39	3577 (52.31, 176.53) 0.17	3564 (356.55, 231.21) 0.15	3353 (8084.55, 0.00) 0.25	ν_s(NH$_2$) a′
40	3589 (54.01, 135.56) 0.17	3549 (92.21, 46.99) 0.56	3474 (3183.38, 229092.49) 0.59	ν(N$_1$H) a′
41	3645 (78.74, 142.33) 0.25	3598 (193.03, 119.90) 0.21	3526 (3296.49, 47670.96) 0.70	ν(N$_9$H) a′
42	3686 (41.09, 66.27) 0.74	3684 (127.86 , 55.89) 0.72	3535 (1708.27, 24858.88) 0.08	ν_{as}(NH$_2$) a′

[a] *The first and second numbers within each bracket represent IR intensity and Raman activity while the numbers above and below each bracket represent the corresponding calculated frequency and depolarization ratio of the Raman band respectively.*

vw: very-weak, w: weak, m: medium, ms: medium-strong, s: strong, vs: very-strong, vvs: very- very strong.

The calculated frequency for out-of-plane mode of NH$_2$ group i.e. torsion mode found to be increases by 130 cm^{-1} and 44 cm^{-1} for the G$^+$ and G$^-$ species with intense band of IR and Raman. The wagging mode of NH$_2$ group lower by magnitude 112 cm^{-1} for the G$^-$ than that of the G while this is equal in magnitude in case of the G and G$^+$ radical. The rocking mode of NH$_2$ found to be decreases by 37 cm^{-1} and scissoring of this increases by 22 cm^{-1} for the G$^+$ radical as compared to the G molecule. The magnitude of the scissoring mode of NH$_2$ group decreases by 60 cm^{-1}. The antisymmetric stretching of NH$_2$ group have to found lower by 160 cm^{-1} for the G$^-$ species and coupled with N$_9$H stretching mode. The magnitude of IR intensity and Raman activity increases in the G$^-$ species than that of the neutral G molecule. The stretching frequencies of the N$_1$H and N$_9$H bonds for the G$^+$ and G$^-$ species calculated to have lower frequencies as compared to the neutral G molecule. The bending mode of NH increases in the G$^+$ species and equal magnitude for the G$^-$ species. Out-of-plane modes of NH also increase by 101 and 88 cm^{-1} for the G$^+$ species as compared to the G molecule. The bending mode of CH decreases by 74 cm^{-1} and out-of-plane mode of C-H increases by 68 cm^{-1} for the G$^+$ species and equal in magnitude of the G$^-$ and G species. Stretching mode of C=O decreases by 35 cm^{-1} for the G$^-$ species and to be nearly equal in the G$^+$ species.

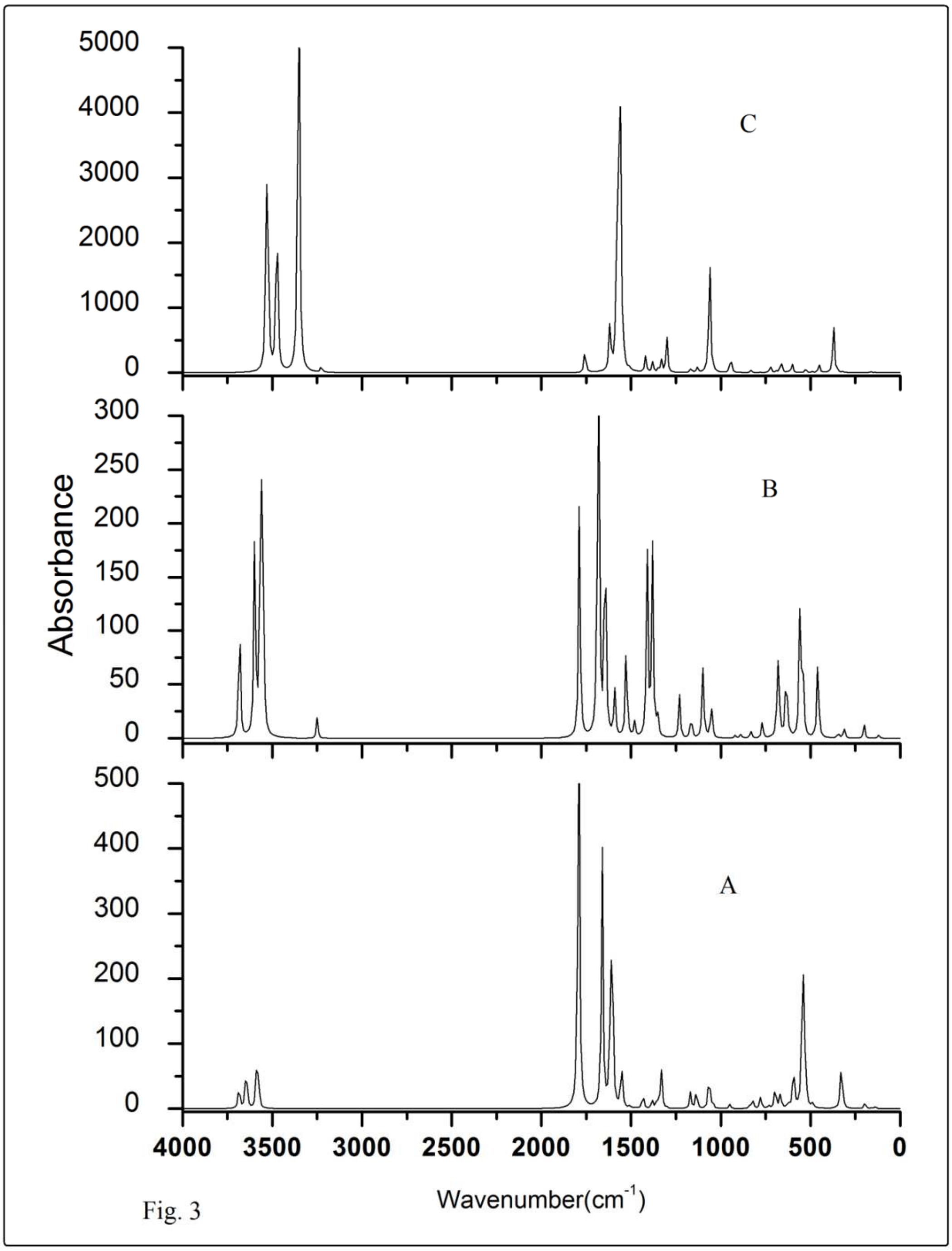

Figure – 3

*A- Calculated IR Spectra of the G molecule at the b3lyp/6-311++g** basis set.*
*B- Calculated IR Spectra of the G^+ molecule at the b3lyp/6-311++g** basis set.*
*C- Calculated IR Spectra of the G^- molecule at the b3lyp/6-311++g** basis set.*

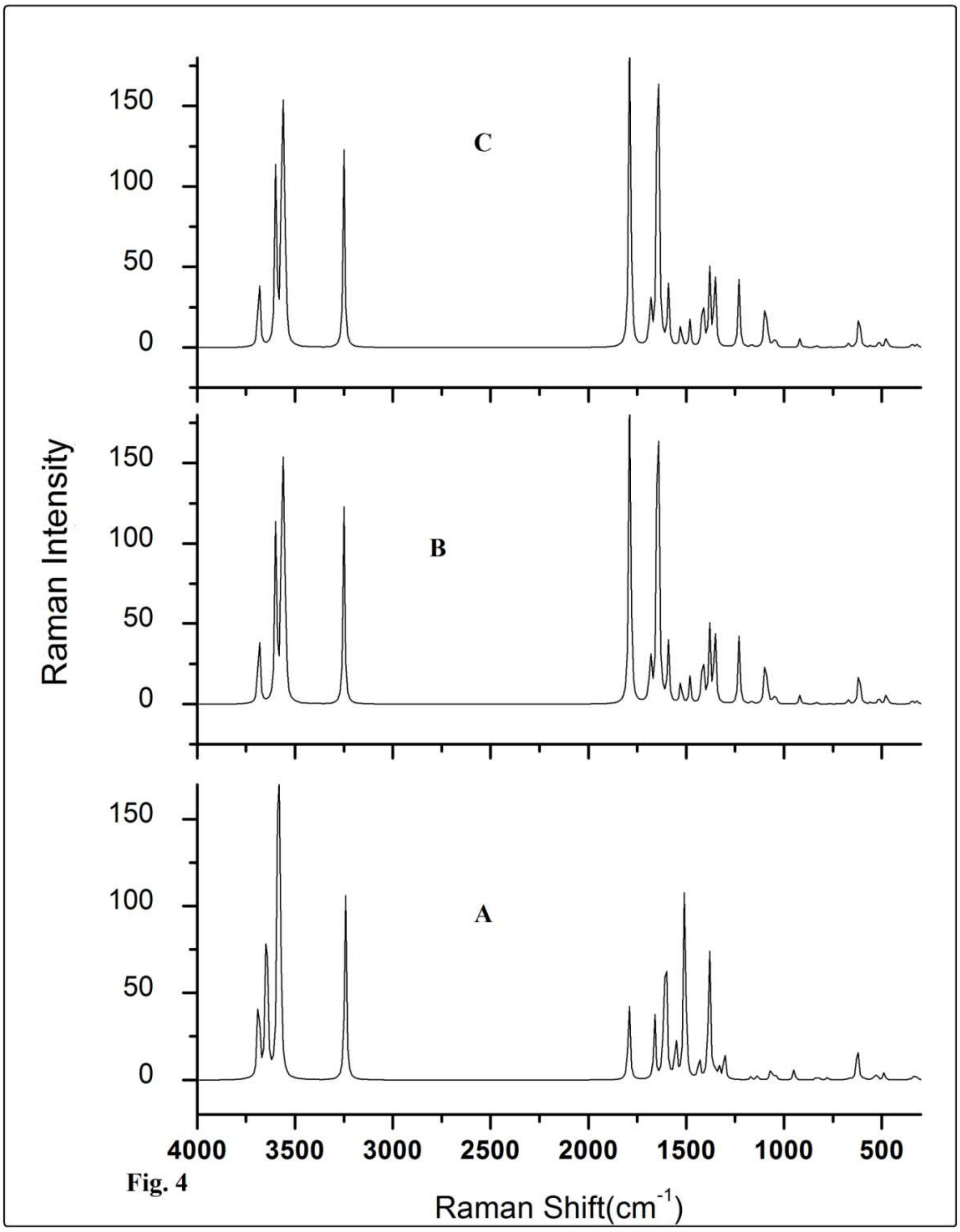

Figure – 4
*A- Calculated Raman Spectra of the G molecule at the b3lyp/6-311++g** basis set.*
*B- Calculated Raman Spectra of the G^+ molecule at the b3lyp/6-311++g** basis set.*
*C- Calculated Raman Spectra of the G^- molecule at the b3lyp/6-311++g** basis set.*

3.3. Other spectroscopically important parameters

Total energies, dipole moments, zero-point vibrational energies and other relevant thermodynamic functions for the neutral G molecule and its radicals calculated at the B3LYP/6-311++G** level are collected in Table-4. The calculated dipole moment, S and rotational constant B and C increase in the G^+ radical while in case of the G^- radical these parameters are going to be decrease. The magnitude of calculated C_V, E and zero point vibrational energy slightly decrease in the G^+ species and vice versa in case of the G^- species. The anionic radical of the G is more stable than the neutral G molecule while the cationic radical of the G is less stable than the neutral G molecule.

Table-4: Calculated Energies, Dipole Moment, Zero-point vibrational and Thermodynamics functions of Guanine and its radicals

	G	G^+	G^-
Total Energies (Hartree)	-542.71358848	-542.43064610	-542.71038889
Zero-point vibrational energy (Kcal/Mol)	72.95649	72.83130	71.69711
μ (Debye)	6.7407	7.1120	4.2303
C_V (Cal/Mol-Kelvin)	32.955	32.824	33.148
S (Cal/Mol-Kelvin)	89.045	90.446	90.402
E (Thermal) (Kcal/Mol)	78.161	78.011	76.914
Rotational Constant(GHZ)			
A	1.91913	1.89564	1.91962
B	1.11309	1.13011	1.11281
C	0.70488	0.70802	0.70473

CONCLUSION

The frequency calculations indicated that they are now at energy minima. The G^+ species favors the planar geometrical structure while the neutral G and G^- species is non-planar symmetric structure. Redistribution of the electrons on the G^+ species the atomic charges of each atom are slightly increases. Both the cationic and anionic radicals of the G molecule are found to be stable. The stretching mode of C=O decreases for the G^- species and to be nearly equal in the G^+ species. For the anionic species of the G molecule, the magnitude of the calculated frequency is nearly same but the IR intensity and Raman activity increases by a large factor.

REFERENCES

[1] G.G. Sheina; S.G. Stepanian; E.D. Radchenko; Yu.P. Blagoi. *J. Mol. Struct.*, **1987**, 158, 275-292.
[2] L. Gorb; A. Kaczmarek; A. Gorb; A.J. Sadlej; J. Leszczynski. *J. Phys. Chem.B*, **2005**, 109,13770-13776.
[3] A. Graslund; A. Ehrenberg; A. Rupprecht; G. Strom; H.Crespi. *Int. J. Radiat. Biol.*, **1975**, 28**,** 313-232.
[4] M. Yan; D. Becker; S. Summerfield; P. Renke; M.D. Sevilla. *J. Phys. Chem.*, **1992**, 96**,** 1938-1950.
[5] S.D. Wetmore; L.A. Eriksson; R.J. Boyd; in: L.A. Eriksson Ed., Theoretical Biochemistry: Processes and Properties of Biological Systems, Theoretical and Computational Chemistry, Elsevier, Amsterdam, **2000**, Vol. 9, and references therein.
[6] J. Leszczynski; in: M. Hargittai; I. Hargittai (Eds.), Advances in Molecular Structure and Research, vol. 6, JAI Press Inc., Stamford, Connecticut, **2000.**
[7] C. E. Bugg; U. Thewalt. *J Am Chem Soc.*, **1970,** 92, 7741-7750.
[8] J. D. Zhang; Y. Xie; H. F. Schaefer. *J Phys Chem* A, **2006**, 110,12010-1216.

[9] K. Szczepaniak; M. Szczesniak; W. Szajda; W.B. Person; J.Leszczynski. *Can. J.Chem.*, **1991,** 69, 1705-1720.

[10] K. Szczepaniak; M. Szczesniak. *J. Mol. Struct.*, **1987,** 156, 29-42.

[11] A. K.Chandra; M.T. Nguyen; T. Uchimaru; Th.Z. Huyskens. *J of Mol Struct.*, **2000**, 555, 61-66.

[12] F. Ortmann; K. Hannewald; F. Bechstedt. *J Phys Chem* B, **2008**, 112, 1540-1548.

[13] O. E. Kasende; K. Szczepaniak; W. B. Person; T. Z. Huyskens. *J of Mol Struct.*, **1997**, 435, 17-33.

[14] O. E. Kasende. *Spectrochimica Acta Part* A, **2002**, 58, 1793-1808.

[15] J. Florian. *J. Phys. Chem.*, **1993**, 97, 10649-10658.

[16] Y. Nishimura; M. Tsuboi; S. Kato; K. Morokuma. *Bull. Chem. Soc. Jpn.*, **1985,** 58, 638.

[17] M.J. Frisch et al. Gaussian 03, Revision C. 02, Gaussian, Inc.,Wallingford, CT, **2004**.

[18]. A. Frisch, A. B. Nielsen, A. J. Holder, GaussView user manual, Gaussian, Inc., Wallingford,USA, **2003**.